Journal of Nuclear Materials 386–388 (2009) 181–184

Contents lists available at ScienceDirect

Journal of Nuclear Materials

journal homepage: www.elsevier.com/locate/jnucmat

Difference between helium retention properties in 316L and 304 stainless steels

Mitsutaka Miyamoto [a,*], Kotaro Ono [a], Yusuke Mori [a,b], Daigo Shitabou [a,c]

[a] Department of Material Science, Shimane University, Matsue, Shimane 690-8504, Japan
[b] Yasugi Works, Hitachi Metals, Ltd., Yasugi, Shimane 692-8601, Japan
[c] Sales Engineering Department, PS Company, Disco Corporation, Tokyo 143-8580, Japan

A B S T R A C T

The difference between helium behavior in type 316L and 304 stainless steels at high temperature was examined. Thermal desorption experiments were performed to obtain fundamental knowledge on the retention properties of helium atoms and in situ TEM observation was also carried out to examine the related dynamic behavior of helium bubbles. The desorption properties indicated that SUS316L has strong retention up to high temperatures. In SUS316L, a large desorption peak was present at temperatures above 1200 K, whereas most of the retained helium was desorbed at comparatively low temperatures in SUS304. In situ TEM observation consistently showed rather lower mobility of bubbles in SUS316L compared with SUS304. The suppression of bubble motion could be caused by Mo atoms, the additive in SUS316L.

1. Introduction

Structural materials of fusion and fission reactors suffer serious damage by irradiation with high dose neutrons. These neutrons generate insoluble helium atoms by (n,α) nuclear reaction, and make the reactor materials brittle. In particular, in the case of repair welding of reactor materials, crack formation is a serious problem even at a helium level of 10 ppm [1–5]. In addition, Morishima et al. reported that the weld cracking susceptibility of neutron irradiated 316L stainless steel (SUS316L) seemed to be higher than that of SUS304 [6]. These studies mentioned the effects of helium bubble formation and growth, however, the reason for the difference in weld cracking susceptibility was not clear. Therefore, for the development of welding techniques for irradiated materials, more information is required on the segregation behavior of helium bubbles at grain boundaries in SUS316L and SUS304. Using thermal desorption spectroscopy (TDS) and in situ transmission electron microscopy (TEM), the present study aimed to obtain fundamental knowledge on the retention properties of helium atoms in austenitic stainless steels and the related dynamic behavior of helium bubbles at high temperature.

2. Experimental procedure

Specimens used in the present study were made from base materials of solute annealed SUS316L and SUS304. Specimens of SUS304L were also used as reference material. The chemical compositions of these specimens are shown in Table 1. The specimens cut from the base materials were mechanically polished to 0.1 mm thick sheets and vacuum-annealed at 900 K for 24 h. After annealing, the specimens were electrochemically polished to remove surface contaminants for TDS. Thin films for TEM observation were punched out from the same sheets and prepared by twinjet-electrochemical polishing with an electrolyte of 5% $HClO_4$ and 95% CH_3COOH.

The specimens were irradiated with 20 keV He^+ at temperatures between R.T. and 673 K, with a flux of about 1×10^{17} He^+/m^2 s and total fluence was controlled from 1×10^{18} to 1×10^{20} He^+/m^2. After the irradiation, thermal desorption of helium was measured quantitatively with a quadrupole mass filter during annealing up to about 1320 K at a constant heating rate of 0.1 K/s. In addition to these thermal desorption experiments, in situ TEM observation during the irradiation and post-annealing was also performed to examine the dynamic behavior of helium bubbles. In cases where bubbles were mobile, the relationship between the mean square of the migration distance, $\langle R^2 \rangle$, and time, t, was analyzed Fig. 5. If a proportional relationship was observed, the diffusion coefficient, D, was estimated using the equation $\langle R^2 \rangle = 4Dt$ according to random walk theory. Details of the method and theories have been given elsewhere [7]. In identifying the bubble positions, the center positions of each bubble were measured from video images with an observational error of less than 0.6 nm.

3. Results and discussion

3.1. Microstructure of irradiated specimens

The microstructural evolution of the specimens was examined at several temperatures under irradiation with 20 keV He^+ in

* Corresponding author.
E-mail address: miyamoto@riko.shimane-u.ac.jp (M. Miyamoto).

0022-3115/$ - see front matter © 2008 Elsevier B.V. All rights reserved.
doi:10.1016/j.jnucmat.2008.12.088

Table 1
Chemical compositions (wt%) of SUS316L, SUS304 and SUS304L.

	C	Si	Mn	*P*	*S*	Ni	Cr	Mo	*B* (ppm)
SUS316L	0.015	0.52	0.96	0.020	0.004	12.39	16.28	2.12	3
SUS304	0.06	0.71	1.06	0.020	0.001	8.44	18.23	–	2
SUS304L	0.015	0.54	0.97	0.027	0.006	10.10	18.60	0.30	–

advance of the thermal desorption experiments. The densities and sizes of helium bubbles were plotted as a function of fluence at each irradiation temperature as shown in Fig. 1. A slight difference in densities arose with increasing irradiation temperature, though little significant difference was observed in the sizes of the bubbles. This seems to indicate that large numbers of tiny bubbles with a size unobservable by conventional TEM still exist in SUS316L even at high temperature due to the lower mobility of vacancies or helium-vacancy complexes. Details of the microstructural evolution under the irradiation will be reported in the near future [8].

3.2. Thermal desorption spectra of helium

The thermal desorption experiments showed the key differences between SUS316L and SUS304. Fig. 2 shows thermal desorption spectra of helium implanted with 20 keV He^+ at room temperature and a fluence of 1.3×10^{19} D/m^2. From the shape of the desorption peaks, three characteristic temperature regions were defined as shown in Fig. 2; region I ranging from 890 to 1000 K, region II from 1000 to 1250 K, and region III above 1250 K.

In region I, a similar low desorption occurred from both specimens. This desorption seemed to be de-trapping from strain fields around dislocation loops, because most dislocation loops had contracted and disappeared by about 1000 K. Fig. 3 shows the shrinkages in SUS316L and SUS304 obtained by in situ observation during the post-irradiation annealing. These shrinkages could be caused by absorption of thermal vacancies which has a formation energy of 1.8 eV in FCC Fe [9]. This kind of desorption related to extinction of I-loops has also been observed in pure Fe and Fe–9Cr ferritic alloy [10].

In region II, significant desorption occurred from SUS304 whereas SUS316L had relatively low desorption. This desorption seemed to be related to the migration of small bubbles because different migration behaviors were observed as described in the next section. This means that bubble migration was suppressed and helium atoms were retained up to rather high temperatures in SUS316L. In region III, a huge desorption peak was present only in SUS316L in contrast to the peak in region II. The helium atoms

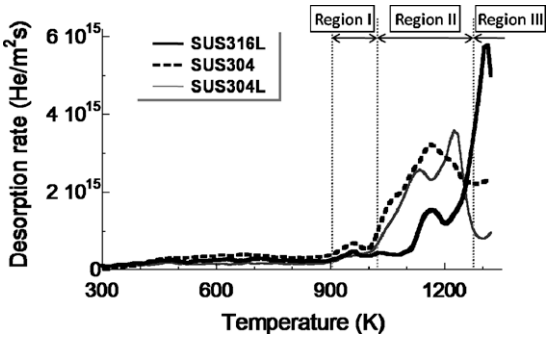

Fig. 2. Comparison of TDS in SUS316L, SUS304 and SUS304L irradiated with 20 keV He^+ and with a fluence of 1.3×10^{19} He^+/m^2 at room temperature.

retained as bubbles in SUS316L finally started to desorb in this temperature region. This stronger retention property of SUS316L was also confirmed from the viewpoint of the total desorbed amount. The amounts which were desorbed from SUS316L and SUS304 during annealing up to 1320 K were about 58% and 80% of the net implanted helium atoms, respectively. This means that many helium atoms are still retained until high temperatures in SUS316L.

The thermal desorption spectrum for SUS304L is also plotted in Fig. 2. It is generally similar to that for SUS304 in that the peak in region II, for instance, started at the same temperature. Additionally, there was no significant difference in the microstructure between SUS304 and SUS304L, which is not shown. This means that carbon within the range of concentrations shown in Table 1 has little influence on the retention property. In other words, the interaction between helium atoms and material damage is so strong that the carbon effect is negligible.

3.3. Dynamic behavior of defect clusters

The dynamic behavior of bubbles obtained by in situ TEM observation, which is inseparably connected to the thermal desorption spectra, promote an understanding of the retention

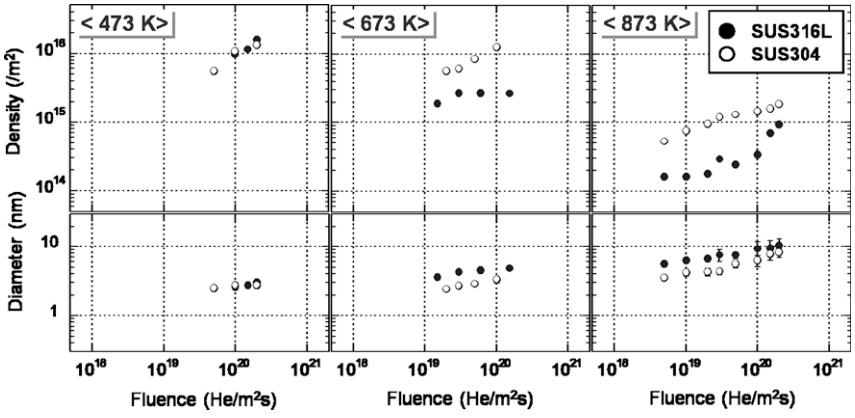

Fig. 1. Fluence dependence of area density and diameter of helium bubbles induced by irradiation with 20 keV He^+ at each temperature.

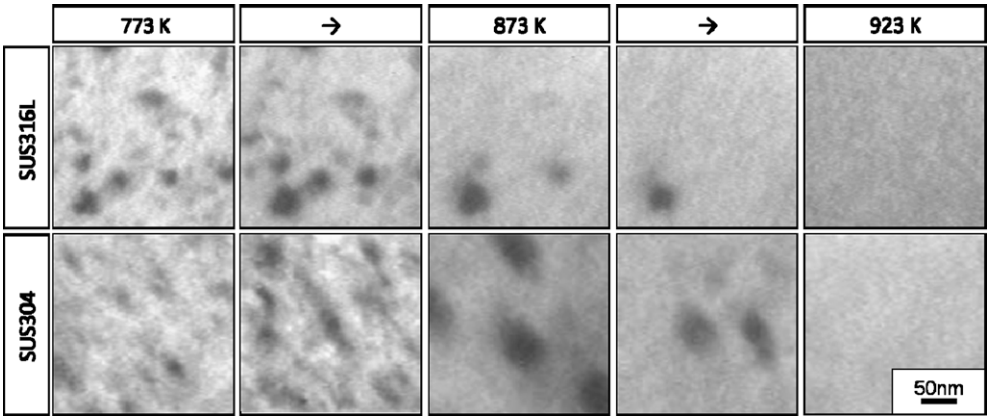

Fig. 3. Microstructure evolution in SUS316L and SUS304 during annealing, following irradiation with 20 keV He^+ and with a fluence of 1.3×10^{19} He^+/m^2 at room temperature. The images show the shrinkage and disappearance of dislocation loops.

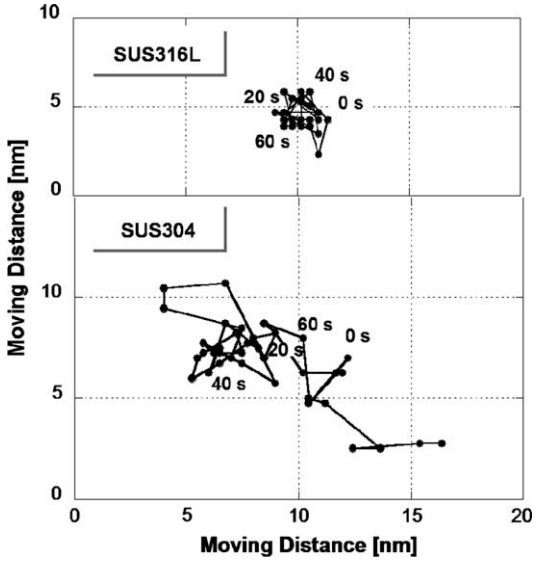

Fig. 4. Trajectories of bubbles with almost the same diameter of 3.5 nm during annealing at 1073 K in SUS316L and SUS304. The positions of the bubbles were plotted every 1 s for 60 s.

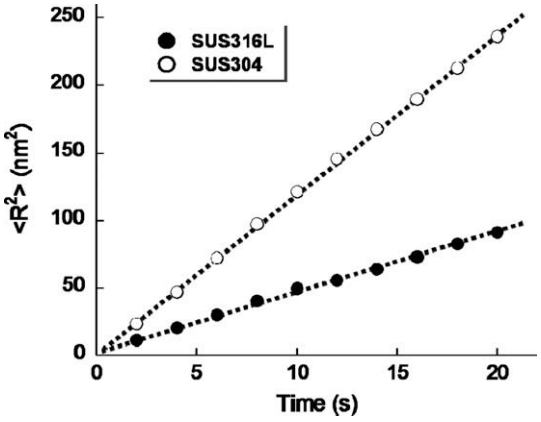

Fig. 5. Mean squares of the bubble migration distance, $\langle R^2 \rangle$, versus time.

mechanism. This observation showed the clear difference in bubble mobility between SUS316L and SUS304.

Fig. 3 shows the trajectories of helium bubbles with almost the same diameter of 3.5 nm during annealing at 1073 K in SUS316L and SUS304. The positions of the bubbles were plotted every 1 s for 60 s. From comparison of the motions shown in this figure, the bubble mobility in SUS316L was clearly suppressed. To compare the behavior of these bubbles quantitatively, the mean squares of the migration distances, $\langle R^2 \rangle$, were analyzed as a function of time. In Fig. 4, data obtained from the bubbles shown in Fig. 3 are plotted. Clearly, these mean squares are proportional to time in both specimens, which indicates Brownian type motion. From the slopes in the figure, $D_{SUS316L} = 1.1 \times 10^{-18}$ m^2/s and $D_{SUS304} = 3.0 \times 10^{-18}$ m^2/s were derived as diffusivity coefficients on the basis of random walk theory. This difference in bubble mobility should cause the difference in thermal desorption properties between SUS316L and SUS304.

Although the precise reason for the difference in bubble mobility cannot be identified in this study, molybdenum, an oversized additive in SUS316L, seems to contribute to suppression of bubble motion. It could be considered reasonable that molybdenum atoms segregating around bubbles suppress diffusion on the medial surface of bubbles. The difference in bubble mobility is one of the most important factors causing the difference in weld cracking susceptibility. Further investigation into the details of the precipitation or segregation properties using, for example, STEM-EDS analysis is required.

4. Summary

The thermal desorption behavior of helium from SUS316L and SUS304, irradiated with 20 keV He^+ ions, has been compared to obtain fundamental knowledge on the retention properties of helium atoms in austenitic stainless steels. Although similar small desorptions attributed to the disappearance of I-loops were observed in both specimen at almost the same temperature, desorption caused by bubble migration occurred at a much higher temperature in SUS316L compared to SUS304. In situ TEM observation during post-irradiation annealing showed rather lower mobility of bubbles in SUS316L as the reason for the difference in retention properties. This suppression of bubble mobility could be caused by molybdenum atoms, the oversized additive in SUS316L.

References

[1] C.A. Wang, M.L. Grossbeck, B.A. Chin, J. Nucl. Mater. 225 (1995) 59.
[2] W.R. Kanne Jr. et al., J. Nucl. Mater. 225 (1995) 69–75.
[3] H.T. Lin, M.L. Grossbeck, B.A. Chin, Metal. Trans. A 21 (1990) 2585.
[4] F. Kano et al., J. Nucl. Mater 228&263 (1998) 2013–2017.

[5] S. Kawano et al., J. Nucl. Mater 228&263 (1998) 2018–2022.
[6] Y. Morishima et al., J. Nucl. Mater 329–333 (2004) 663–667.
[7] K. Ono, S. Furuno, S. Kanamitsu, K. Hojou, Philos. Mag. Lett. 75 (1997) 59.
[8] M. Miyamoto, K. Ono, et al., in preparation.
[9] K. Morishita et al., Fusion Sci. Technol. 44 (2003) 441–445.
[10] K. Ono et al., J. Nucl. Mater 329–333 (2004) 933–937.